Critical phenomena in amorphous ferromagnetic and spin-glass alloys

Y. Yeshurun, M. B. Salamon, and K. V. Rao*
Department of Physics and Materials Research Laboratory, University of Illinois at Urbana-Champaign, Urbana, Illinois 61801

H. S. Chen
Bell Laboratories, Murray Hill, New Jersey 07974
(Received 17 February 1981)

Four amorphous alloys of the type $(T_{1-x}T'_x)_{75}P_{16}B_6Al_3$ with transition metal T = Fe or Co and T' = Mn or Ni are studied by low-field ac susceptibility bridge and vibrating sample magnetometer techniques. All systems under study have a ferromagnetic (FM) behavior for low concentrations x of T' and a spin-glass (SG) behavior for high x. In the intermediate concentration regime alloys are characterized by a sharp drop in the ac susceptibility below the Curie temperature, at a temperature T_d, and by a vanishing of the magnetization at a lower temperature $T_{FG}(x)$ which we identify as a transition temperature. Critical exponents have been extracted for the paramagnetic (PM)-FM and for the FM-SG transitions by using a scaling procedure. The PM-FM critical exponents have non-Heisenberg values ($\beta = 0.4$ and $\delta = 5$), while the FM-SG critical exponents seem to depend on x. The PM-SG line can also be viewed as a critical line as the peaks in the susceptibility obey scaling laws. Thus, we can identify for each system three lines of transitions intersecting at a multicritical point (MCP). The phase diagram and the nature of the MCP are similar to the predictions of the Sherrington-Kirkpatrick model.

I. INTRODUCTION

Study of models[1] proposed to explain spin-glass behavior imply more complex properties of the phase diagram whenever the mean of the distribution of exchange energies becomes comparable to its width. In such random systems, the ferromagnetic phase-transition line is predicted to intersect lines bounding the spin-glass phase at a multicritical point.

Although the models which predict this type of phase diagram are subject to serious criticism,[2] a number of materials have been found which exhibit such an interplay of phases. Based on ac susceptibility data, the systems $Fe_{3-x}Al_{1+x}$,[3] $(PdFe)_{1-x}Mn_x$,[4] $(Fe_{1-x}Ni_x)_{75}P_{16}B_6Al_3$,[5] and $(Fe_{1-x}Mn_x)_{75}P_{16}B_6Al_3$ (Ref. 6) were reported to show a change from ferromagnetism to spin-glass behavior over some range of composition. The interpretation of the drop in ac susceptibility as evidence for a change of phase has been disputed,[7] but it is nonetheless accepted that the ferromagnetic phase may be reentrant, by which we mean that it gives way to a nonferromagnetic phase at low temperatures. A considerable body of evidence has been amassed for the $Eu_{1-x}Sr_xS$ system,[8] that indicates a ferromagnetic-spin-glass multicritical point (MCP). Here, suggestions of spinodal decomposition and chemical clustering blur the issue.[9] Quite recently, evidence has been presented for reentrant behavior in Fe_xCr_{1-x} (Ref. 10) and $(Fe_{1-x}Ni_x)_{75}P_{16}B_6Al_3$ (Ref. 11) systems based on the temperature dependence of the neutron scattering intensity and the spin-wave stiffness constant. Reentrant behavior in the latter system was detected also by means of ferromagnetic resonance experiments.[12]

Although it is now clear that the ferromagnetic phase may be reentrant, and that a MCP might exist, clear identification of the nature of the phase transition between ferromagnet and spin-glass has been lacking. Recently,[13] we demonstrated that such a line of phase transitions does indeed occur, and extracted the critical exponents. The system reported there is a series of amorphous alloys with composition $(Fe_{1-x}Mn_x)_{75}B_{16}P_6Al_3$. Amorphous alloys offer several distinct advantages for the study of random magnetism not realizable in compounds or ordered alloys. Among these are the following: (i) All compositions are possible within the amorphous phase. (ii) The structure of the liquid phase is quenched in, thereby largely avoiding solid-state clustering and segregation. (iii) There are no grain boundaries or lattice imperfections at which magnetic ions can cluster, or which can pin domain boundaries. (iv) Any magnetocrystalline anisotropy present will also be random. We claim these alloys represent, to the extent possible, a physical realization of a bond-random, quenched magnetic system.

In this paper, we report details of the phase diagrams, critical, and multicritical behavior of four alloys of the type $(T_{1-x}T'_x)_{75}B_{16}P_6Al_3$, where T is Fe or Co and T' is Ni or Mn. This is in fact the first sys-

tematic study of critical behavior of ferromagnetic and spin-glass phases in these alloys. We find considerable similarity among these four alloy systems and in general, these results confirm our previous studies on Fe-Mn. In all alloys we can identify a multicritical point. However, the Ni alloys are found to have multicritical points at much higher values of x than the corresponding Mn alloys. Thus, the Ni alloys and the Mn alloys represent dilute and concentrated spin-glass systems, respectively. The critical behavior along the paramagnetic-ferromagnetic line in the four alloys is similar to that reported previously for other amorphous alloys. The location of the ferromagnet-spin-glass line necessitates a reanalysis of our previous study[6] of the susceptibility along the spin-glass–paramagnetic line. We show that scaling continues to hold, but that the susceptibility exponent must be slightly reduced.

In Sec. II of this paper, we review the results of Sherrington-Kirkpatrick-type models as they apply to the phase diagram and critical exponents of a random magnet. A description of the experimental procedure, Sec. III, is followed by detailed descriptions of the phase diagrams for the four alloys in Sec. IV. In succeeding sections, the critical behavior along each of the phase boundaries is discussed in turn: the ferromagnet-paramagnet line in Sec. V, the ferromagnet–spin-glass line in Sec. VI and the spin-glass–paramagnet line in Sec. VII. Finally, a summary and discussion of the results follows in Sec. VIII.

II. SPIN-GLASS AND FERROMAGNETIC PHASE BOUNDARIES

In this section we discuss theoretical results for the phase diagram and critical behavior of a magnetic material containing a random mixture of ferromagnetic and antiferromagnetic interactions. In contrast with an orderly mixture of interactions, which give rise to spiral and other periodic spin structures, a solution for the random problem is not known.

The first suggestion that a transition to a low-temperature state might occur was made by Edwards and Anderson (EA).[14] They proposed a ground state consisting of randomly oriented, but stationary, spins, whose order parameter is given by the spatial average of the square of the thermal-average magnetization. Following that suggestion, Sherrington and Kirkpatrick (SK)[1] proposed a "soluble" model which has an EA ground state over a certain range of values for the ratio $\tilde{J}_0/\tilde{J}$, where $\tilde{J}_0$ is the mean value and $\tilde{J}$, the standard deviation (second cumulant moment) of the distribution of J_{ij}, the pair exchange constant. The SK solution, which involves the so-called replica trick, leads to the phase diagram shown in Fig. 1. A number of unphysical features of the solutions,

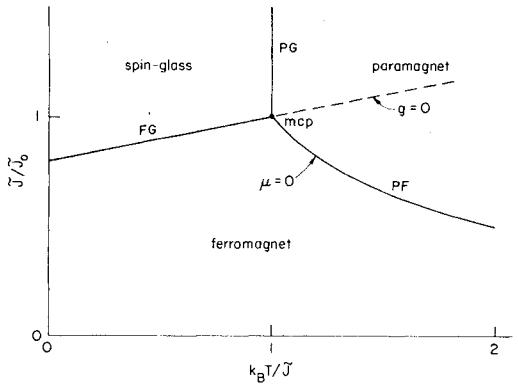

FIG. 1. Magnetic phase diagram in the Sherrington-Kirkpatrick model. The critical lines are labeled as referred to in the text. Also shown the scaling fields μ and g.

mainly a negative entropy at $T=0$ K, have led to a variety of alternative solutions, all of which yield similar results. A summary of such mean-field solutions to the SK problem has been given by Bray and Moore,[2] along with a critique of "second-generation" solutions which involve multiple order parameters. One approach[15] which differs from the rest employs Migdal-Kadanoff real-space methods for a two-δ function distribution of J_{ij}, and leads to a similar phase diagram to Fig. 1, but with nonclassical critical exponents

In order to discuss the behavior of the magnetization along the various lines in Fig. 1, it is useful to consider the Landau-Ginzburg-Wilson functional introduced by Chen and Lubensky,[16] For a one-component (Ising) spin system, this is

$$F(H,T)=\tfrac{1}{2}r_m M^2-\tfrac{1}{4}r_q Q^2-2wQ^3 + w_1 M^2 Q+vM^4-MH \ , \quad (1)$$

where $r_m=(k_BT/\tilde{J}_0-1)$ and $r_q=[(k_BT/J)^2-1]$. On minimizing Eq. (1) with respect to M and Q (where Q is the EA order parameter), one obtains the following picture:

(i) Along $r_q \simeq 0$ for $r_m>0$: $Q=0$ for $r_q>0$ and $Q=-r_q/12w$ for $r_q<0$; $M=0$ on both sides of the boundary. The magnetic susceptibility is given by $\chi_m \propto r_m^{-1}$ in the P (paramagnetic) phase and $\chi_m \propto r_m^{-1}+w_1 Q$ in the SG phase, displaying the well-known cusp. We label this line PG.

(ii) Along $r_m \simeq 0$ and $r_q>0$: $Q \propto -r_m$ and $M \propto (-r_m)^{1/2}$ in the ferromagnetic (FM) phase. χ_m diverges along this line as r_m^{-1}; we call this the PF line.

(iii) Along $r_q/r_m \cong 6w/w_1$: Q is continuous while $M \propto (r_q/r_m-6w/w_1)^{1/2}$ in the FM phase. Along this phase boundary $\chi_m \propto (r_q/r_m-6w/w_1)^{-1}$, and we call

this line the FG line.

(iv) At the multicritical point $r_m = r_q = 0$: for a path approaching the MCP from the FM phase, but not along the phase boundary, $M \propto r_m$.

These results may be summarized by a set of critical exponents for each of the critical lines. We label the PF exponents by the usual Greek letters, those along the FG line with tildes, and those for the multicritical point with a subscript t (not to be taken as an ordinary tricritical point). These are summarized in Table I. Along the PG line, the magnetic properties do not show simple power-law dependences in this model.

The value of the crossover exponent ϕ may be obtained by writing Eq. (I) in the scaling form

$$F = r_m^3 f(r_q/r_m, H/r_m^2) \ , \tag{2}$$

valid close to the multicritical point. This is to be compared with ordinary multicritical point scaling,

$$F = r_m^{2-\alpha_t} f(r_q/r_m^{\phi}, H/r_m^{\beta_t \delta_t}) \ , \tag{3}$$

from which we can identify $\phi = 1$.

Attempts to evaluate the exponents beyond the mean-field approximation for the MCP and along the FG line have not been notably successful. The real-space methods of Wortis, *et al.*[15] give a crossover exponent $\phi = 0.955$ for a one-component, three-dimensional random spin system. The specific-heat exponent is $\alpha_t = -1.88$, much smaller than the value $\alpha_t = -1$ obtained from Eqs. (2) and (3) above. No value for the order-parameter exponent was obtained. Conventional renormalization expansions in $6 - d$ lead to complex exponents and indicate that $d = 4$ is the lower critical dimensionality for the SK model.[1] Recent suggestions that the symmetry between replicas may be broken have been explored by Bray and Moore,[2] who suggest that an additional "broken-replica" phase may occur on the ferromagnetic side of the phase boundary, and that this phase must be considered in determining the multicritical properties.

At the present stage, therefore, we must be guided by the mean-field phase diagram and determine the critical exponents empirically. To do this, we have made a series of scaling hypotheses regarding the magnetization within the various phases. This is necessarily incomplete, since the topology of the phase diagram is not known. We adopt the assumption that changes in composition of the alloys affects both $\tilde{J}_0$ and $\tilde{J}$ smoothly and that each composition corresponds to a given ratio of $\tilde{J}_0/\tilde{J}$ and a given temperature scale. We write consequently that there are three boundaries in the temperature-composition plane given by $T_f(x)$, $T_c(x)$, and $T_{FG}(x)$ for the spin-glass–paramagnetic (PG), ferromagnetic-paramagnetic (PF), and ferromagnetic–spin-glass (FG) transitions, respectively. The quantity x is the fractional concentration of one transition metal in the alloy series $(T_{1-x}T'_x)_{75}P_{16}B_6Al_3$. Along the PF boundary, we shall use the scaling form[17]

$$M(H,T) = t^{\beta} m^*(H/t^{\beta\delta}) \ , \quad t = T/T_c(x) - 1 \ . \tag{4}$$

Along the FG line, we take the corresponding form

$$M(H,T) = \tilde{t}^{\tilde{\beta}} m^*(H/\tilde{t}^{\tilde{\beta}\tilde{\delta}}) \ , \quad \tilde{t} = 1 - T/T_{FG}(x) \ . \tag{5}$$

For the PG boundary, the field has no critical effect so that the scaling analysis deals with the approach to the multicritical point. This involves scaling the ac susceptibility rather than the magnetization, which takes the form

$$\chi = g^{-\gamma_t/\phi} \chi^*(\mu/g^{1/\phi}) \ , \tag{6}$$

g and μ are suitable scaling fields to be defined in Sec. VII. The corresponding phase diagram is described in Fig. 1.

Along the boundaries of the FM phase, the magnetization vanishes and the susceptibility is infinite, but both have normal power-law critical behavior. Within the FM phase, however, the magnetization must have a maximum at low fields. This is not easily explored from the scaling approach, but can be examined within the SK model. We have, consequently solved the SK equations with a magnetic field present, with the results shown in Fig. 2 for which

TABLE I. Mean-field values and experimental (average) values of the critical exponents. Experimental values and error bars represent the range of acceptable collapsing of all data points.

	β	δ	$\tilde{\beta}$	$\tilde{\delta}$	β_t	γ_t	δ_t	ϕ
MFA	0.5	3.0	0.5	3.0	1.0	1.0	2.0	1.0
Expt	0.4 ±0.04	5.0 ±0.4	(0.42)	(4.4)	0.4 ±0.05	1.1 ±0.1	2.2 ±0.4	0.77 ±0.05

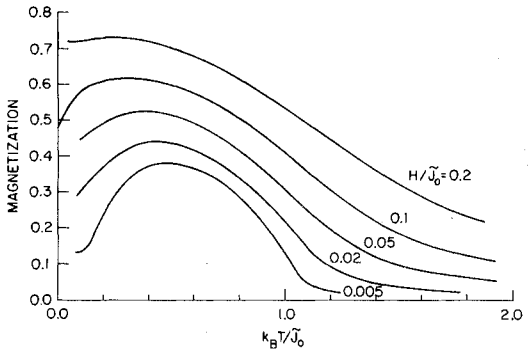

FIG. 2. Magnetization vs temperature for different external magnetic fields in the Sherrington-Kirkpatrick model with $\tilde{J}_0/\tilde{J}=1.1$.

$\tilde{J}_0/\tilde{J}=1.1$. These curves are, as we shall see, more symmetrical than the experimental results, but qualitative agreement lends weight to our assertion that these amorphous alloys closely approximate a SK-like spin-glass–ferromagnetic system.

III. EXPERIMENTAL METHODS

The materials chosen for the present study are amorphous alloys with the composition $(T_{1-x}T'_x)_{75} \times P_{16}B_6Al_3$, where T stands for the transition metals Fe or Co and T' stands for Mn or Ni. In Table II we summarize the samples under study in this review. Alloys were prepared by centrifugal spin quenching.[18] The samples prepared by this technique are in the form of long ribbons with cross section of ~ 1 mm $\times 25$ μm. Rapid quenching preserves the liquid state of the melt thus avoiding possible chemical clustering effects. Also, crystal-field, magnetocrystalline anisotropy, and grain boundary effects are minimized in these amorphous materials. Compositions were generally determined by the proportions of starting materials, but for a few alloys, scanning-electron-microprobe analysis was used to check the nominal concentration x.

Ribbons of the amorphous alloys were cut to approximately 3-mm lengths and packed in the coil of an ac susceptibility bridge, with the longer dimension along the coil axis. The ac susceptibility signal was usually measured at 400 Hz. A check of several frequencies between 100 Hz and 3 kHz showed only a slight dependence of the signal amplitude on frequency. The $\chi(T)$ characteristics (cusps, transition temperatures, etc.), were found to be frequency independent. Data taken both during warming and cooling were completely reproducible. Most of the differential susceptibility measurements were done in zero external magntic field. However, $\partial M/\partial H$ measurements as a function of a dc magnetic field have proven to be a useful tool for separating and identifying the SG and FM transitions close to the multicritical point. For this purpose the sample was centered in an external coil operated by a dc current supply with the ac and dc fields parallel and along the sample axis.

For measurements of the magnetization we used a vibrating sample magnetometer (VSM) with external fields ranging from 10 G to 15 kG. Ten to 20 ribbons of the alloys were cut to approximately 5-mm lengths and placed in the VSM, orientated to minimize the demagnetization factor. After zero-field cooling the sample to He temperature, isotherms of M vs H were taken in order of increasing temperature. Special attention was given to avoiding remanence effects. If remanent magnetization was detected after reducing the field to zero, the sample was heated until the remanence completely disappeared and then cooled again in zero field to the desired temperature.

IV. PHASE DIAGRAMS

In this section we summarize experimental results with magnetic phase diagrams for the $(T_{1-x}T'_x)_{75}P_{16}B_6Al_3$ systems under study. The four systems can be classified with respect to the magnetic properties of the components T and T'. The moment of Fe is least affected by the addition of the glass forming elements (P,B,Al). Ni appears, to a first approximation, to act as a weakly paramagnetic diluent in the mixed transition alloys.[5,19] In the following we demonstrate that despite the differences between these components, the phase diagrams are very similar and exhibit the basic characteristics of the SK phase diagram, Fig. 1.

A. $(Fe_{1-x}Mn_x)_{75}P_{16}B_6Al_3$ system

The ac susceptibility for $x > 0.36$ shows[6] the characteristic spin-glass cusps, which define the freezing temperatures. As x is reduced the temperature of the peak and its amplitude increase. At $x=0.36$ the cusp amplitude of the ac susceptibility signal equals approximately D^{-1} (where D is the demagnetization factor). For $x < 0.36$ a ferromagnetic transition was found at a temperature $T_c(x)$. The Curie temperatures were estimated from the inflection point of the ac signal intensity. Below T_c the ac susceptibility signal saturates at the inverse of the dc magnetization factor D^{-1}. However, this constant value does not persist at low temperatures as is expected for normally behaved ferromagnets. The susceptibility signal starts dropping at temperature $T_d < T_c$. The drop from the "infinite" FM susceptibility signals a change in the development of the spontaneous mag-

TABLE II. Transition temperatures and critical exponents for $(T_{1-x}T'_x)_{75}P_{16}B_6Al_3$ alloys studied in the present work. Experimental values and error bars represent the range of acceptable collapsing of all data points.

T	T'	x	T_c	$T_f(T_{FG})$	β	δ	$\tilde{\beta}$	$\tilde{\delta}$
Fe	Mn	0.20	293 ± 4	(14 ± 2)	0.40 ± 0.03	5.1 ± 0.3		
		0.30	107 ± 2	(31 ± 2)	0.40 ± 0.04	5.0 ± 0.3	0.4 ± 0.03	4.5 ± 0.3
		0.32	100 ± 2	(38 ± 2)	0.40 ± 0.03	5.3 ± 0.3	0.4 ± 0.03	4.5 ± 0.03
		0.36	42 ± 2	42.0	0.40 ± 0.05	2.5 ± 0.5		
		0.44		29.5				
		0.47		28.6				
		0.53		27.3				
		0.59		24.9				
Fe	Ni	0.20[a]	600 ± 4		0.35 ± 0.03	4.3 ± 0.4		
		0.60[a]	334 ± 4		0.40 ± 0.03	5.0 ± 0.4		
		0.65[a]	281 ± 3		0.40 ± 0.04	5.0 ± 0.4		
		0.75[a]	149 ± 3	(18)	0.40 ± 0.04	5.0 ± 0.4		
		0.80	90 ± 3	(21 ± 2)	0.40 ± 0.04	5.0 ± 0.4	0.48 ± 0.6	3.6 ± 0.6
		0.83		32				
		0.85		25.1				
		0.86		20				
		0.90		18				
		0.92		15				
Co	Mn	0.20	298 ± 3	(< 10)	0.40 ± 0.03	5.2 ± 0.4		
		0.30	110 ± 2	(38 ± 3)	0.40 ± 0.04	5.0 ± 0.4	0.38 ± 0.05	4.8 ± 0.6
		0.40		50				
		0.45		80				
		0.50		90				
Co	Ni	0.40	265 ± 4		0.42 ± 0.04	5.0 ± 0.4		
		0.50	182 ± 2	(< 6)	0.38 ± 0.03	5.0 ± 0.4		
		0.60	84 ± 2	(13 ± 6)	0.40 ± 0.04	5.0 ± 0.3		
		0.62	54 ± 2	(13 ± 6)	0.40 ± 0.04	5.3 ± 0.4		
		0.64	38 ± 3	(15 ± 4)	0.40 ± 0.03	5.1 ± 0.3		
		0.66	28 ± 2	(15 ± 4)	0.40 ± 0.04	5.0 ± 0.4		
		0.68	19 ± 2		0.40 ± 0.04	4.0 ± 0.4		
		0.70		16				
		0.72		11				
		0.74		8				
		0.80		6				

[a]Analysis done on unpublished data kindly made available to us by E. Figueroa and K. Gramm.

netization which—as we are able to demonstrate with the dc magnetization measurements—is a characterisitc of a FM-SG transition. These results were presented in Ref. 6. Note that in the present work the values for the Mn concentration are slightly modified due to independent determination by microprobe analysis.

In Ref. 13 we showed magnetization versus temperature curves for the Fe-Mn alloys in different fields. The most striking feature, which is clearly seen in Fig. 1 of Ref. 13, is the maximum in the magnetization curves for low fields. The temperature T_m of the maximum is a decreasing function of the magnetic field and depends on concentration. At higher magnetic field the maximum disappears and a saturation behavior is found. The magnetic field required to wash out the maximum decreases with decreasing x. Even for fields as high as 2 kG a decrease in $M(T)$ is found at low temperature for $x=0.32$; however, for $x=0.2$ this decrease disappears totally above 300 G. This behavior is quite similar to that predicted by the Sherrington-Kirkpatrick model (Fig. 2). The temperature T_m for the lowest field used coincides approximately with T_d,

the temperature at which the ac susceptibility starts dropping from the "infinite" value. Below T_m remanent magnetization appears and the coercive field increases. (As has been noted by others, ac data are difficult to interpret for hysteretic ferromagnets.[7]) At still lower temperatures the remanence increases and time-dependent effects appear. These phenomena suggest the existence of a spin-glass phase. Thus, the combined ac and dc measurements indicate the presence of three phases: paramagnetic, FM, and SG phases at this composition. In Secs. V and VI we will demonstrate that there is a continuous transition from the PM to the FM and from the FM to the SG phase and will locate the exact transition temperatures. In Fig. 3(a) we summarize the experimental results of Refs. 6 and 13 with a phase diagram which consists of three lines of transitions, namely, PF, FG, and PG lines which intersect at a multicritical point. The MCP has been shifted to a higher temperature than that of a previous estimate. Note that the PF line is linear with x for the concentrations under study (T_c below room temperature).

B. $(Fe_{1-x}Ni_x)_{75}P_{16}B_6Al_3$ system

Susceptibility measurements on the Fe-Ni alloys reveal results which are very similar to those described in Sec. IV A. For low concentrations of Ni ($x < 0.65$) the characteristic increase to D^{-1} is observed at T_c. But for intermediate values ($0.65 < x < 0.83$) the ac signal drops at some lower temperature $T_d(x)$. For $x \gtrsim 0.83$ typical SG cusps are observed. However, unlike the sharp cusps in Fe-Mn alloys, these are rounded. By application of a magnetic field, we resolve two peaks in the susceptibility signal which shift apart with increasing field (Fig. 4). In Sec. VII we use scaling analysis to show that these peaks might be related to a FM and a SG transitions with $T_c \simeq T_{FG}$ (alloy concentration close to the MCP).

Magnetization measurements on these alloys in the reentrant regime yield a maximum of M at low fields and give evidence for two transitions: from PM to FM and from FM to SG phases (see analysis in Secs. V and VI). Some characteristic data are plotted in Fig. 5 for $x = 0.8$ The experimental results are summarized by the phase diagram of Fig. 3(b). The PF line is approximately linear with x. The MCP occurs at smaller Fe concentrations and at lower temperatures than in the Fe-Mn system. It is useful to point out that we did not observe changes in the magnetic properties and in the phase diagram of the Fe-Ni system when ^{10}B atoms were replaced by the isotopes ^{11}B for use in neutron scattering work.

C. $(Co_{1-x}Mn_x)_{75}P_{16}B_6Al_3$ system

Analogous to the Fe-Mn system, SG phase is observed for $x \geq 0.4$. However, the ac susceptibility which drops off sharply below T_F, exhibits a considerable broadening of the peak together with a hump (Fig. 6). The freezing temperature is found to increase with x while the intensity of the broad peak drops sharply with increasing Mn concentration. In the intermediate range ($0.2 \leq x \leq 0.3$) two transitions are observed. Typical magnetic measurements

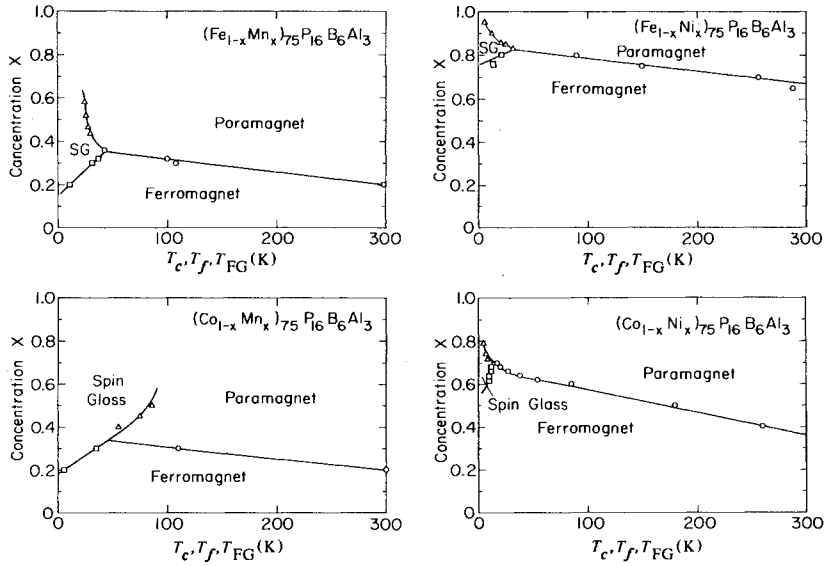

FIG. 3. Magnetic phase diagram for $(T_{1-x}T'_x)_{75}P_{16}B_6Al_3$ systems: (a) Fe-Mn, (b) Fe-Ni, (c) Co-Mn, and (d) Co-Ni.

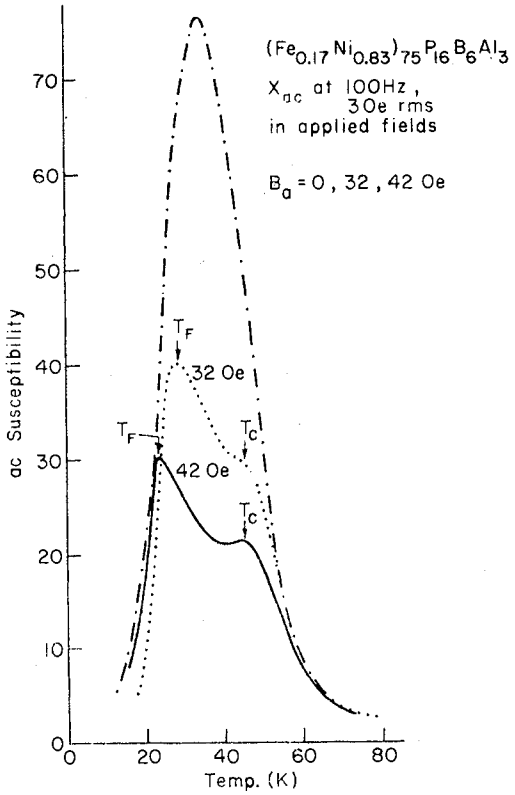

FIG. 4. Low-field ac susceptibility for $(Fe_{0.17}Ni_{0.83})_{75}P_{16}B_6Al_3$ with an without external dc field.

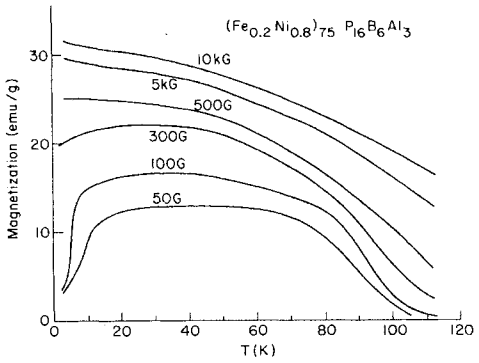

FIG. 5. Isochamps magnetization curves for $(Fe_{0.20}Ni_{0.80})_{75}P_{16}B_6Al_3$.

in this regime are shown in Fig. 7, and the phase diagram, in Fig. 3(c). Note the linearity of the PM-FM line and the unusual positive slope of the SG line. Similar behavior was found in CoMn crystals.[20] Note also that the multicritical point is at approximately the same concentration as for the Fe-Mn system.

D. $(Co_{1-x}Ni_x)_{75}P_{16}B_6Al_3$ system

Susceptibility measurements (Fig. 8) and typical magnetization data[21] (Fig. 9) reveal the same features as for other alloys above. It is interesting to note

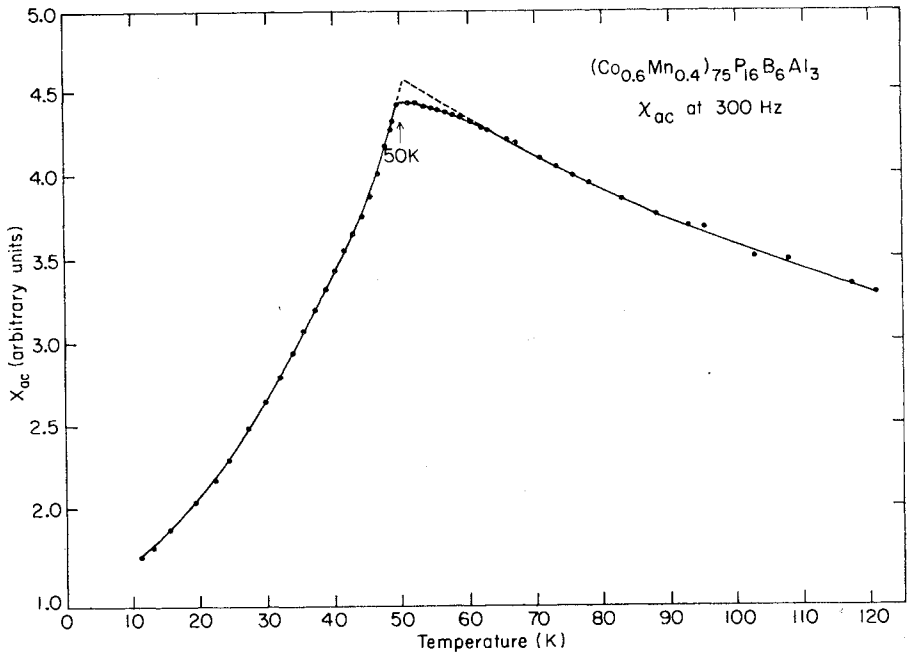

FIG. 6. Low-field ac susceptibility for $(Co_{0.60}Mn_{0.40})_{75}P_{16}B_6Al_3$.

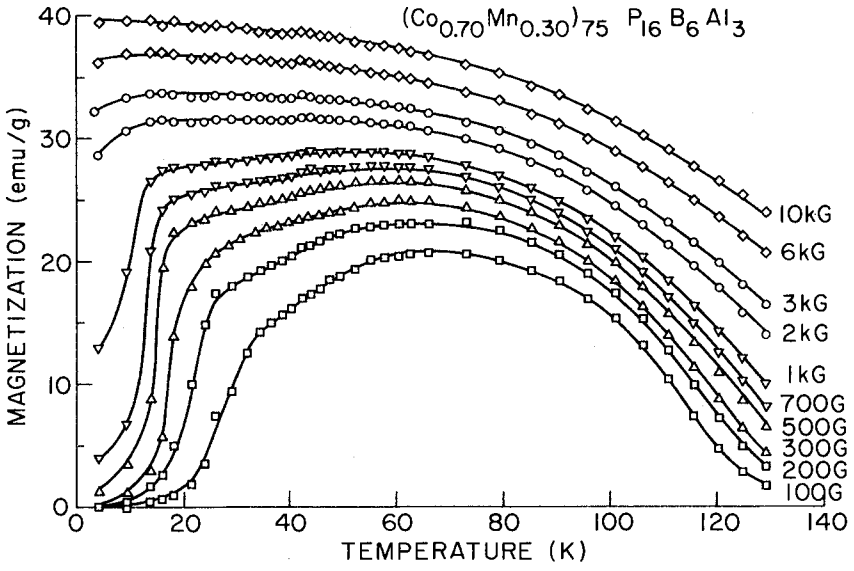

FIG. 7. Isochamp magnetization curves for $(Co_{0.70}Mn_{0.30})_{75}P_{16}B_6Al_3$.

that the SG cusps are rounded as in the Fe-Ni system. dc external fields are used with ac susceptiblity measurements to separate FM and SG transitions for concentrations sufficiently close to the MCP. The experimental results are summarized in the phase diagram of Fig. 3(d). The PF line is linear in most of the studied temperature regimes, with, however, a change in slope near the MCP. The MCP occurs at lower Co concentrations relative to the CoMn system, closer to the value of x_{MCP} in Fe-Ni.

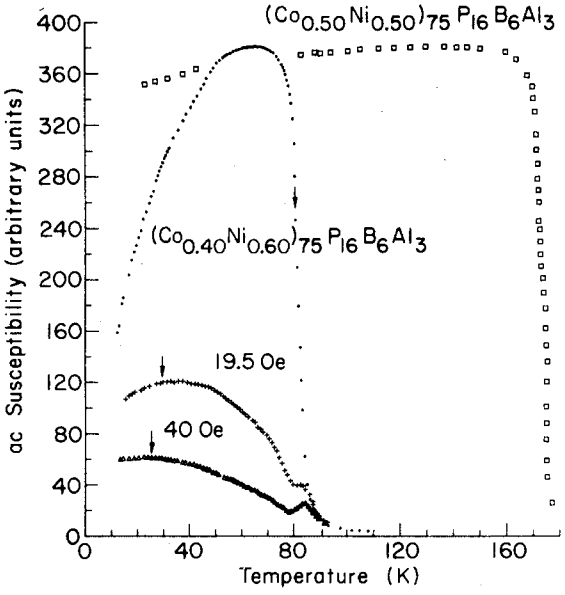

FIG. 8. Low-field ac susceptibility vs temperature for Co-Ni alloys ($x=0.50$ and 0.60). External dc magnetic fields split the rounded cusp ($x=0.60$) to two peaks.

V. PARAMAGNETIC-FERROMAGNETIC LINE

The second order PM-FM phase transition is characterized by a set of critical exponents, β, γ and δ for our purposes defined by

$$M_s \sim t^{\beta} \quad (t<0) \ ,$$
$$\chi \sim t^{-\gamma} \quad (t>0) \ , \tag{7}$$
$$M \sim H^{1/\delta} \quad \text{(critical isotherm)} \ ,$$

where $t \equiv T/T_c - 1$.

A conventional technique for determining critical behavior is given by the modified Arrott plot, namely, plotting $M^{1/\beta}$ vs $(H/M)^{1/\gamma}$ with the proper exponent values to give straight lines. However there is no *a priori* reason to choose one set of exponents or another, and this method is not sensitive enough for accurate determination of the exponents. In the present work we examine the FM critical behavior by using scaling laws, which exploit the relationship $\gamma=\beta(\delta-1)$ between the exponents and a simple form of the magnetic equation of state in the critical region, given by Eq. (4). By defining $y \equiv \mathrm{sgn}(t) \times (H/|t|^{\beta\delta})$, we obtain

$$M(H,T) = t^{\beta} m^*(y) \ . \tag{8}$$

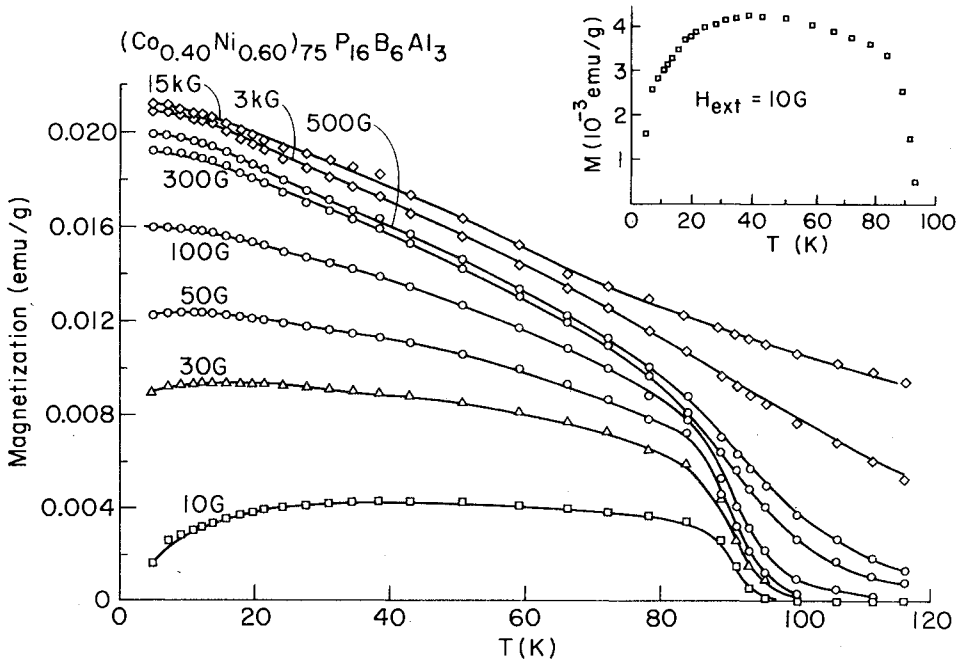

FIG. 9. Isochamp magnetization curves for $(Co_{0.40}Ni_{0.60})_{75}P_{16}B_6Al_3$. Inset shows the magnetization for $H_{ext}=10$ G.

The scaling function m^* has two branches, m_+^* for $t>0$ and m_-^* for $t<0$. The asymptotic behavior for a critical point is described by

$$\lim_{y\to 0} m_-^* = \text{const} \ ,$$
$$\lim_{y\to\infty} m_\pm^* = y^{1/\delta} \ , \qquad (9)$$
$$\lim_{y\to 0} m_+^* = y \ .$$

Thus, by choosing the correct parameters T_c, β, and δ all the data points $M(H,T)$ should collapse to two branches in an M/t^β vs y plot. We find that the best set of parameters—that set which shows the best collapsing to the two branches described by Eqs. (8) and (9)—is unique within the stated error. This means that within reasonable limits ($2\leq\delta\leq 6$, $0.30\leq\beta\leq 0.50$, $T_c\pm 10\%$) we could find no better or equivalent set. The error bars mark the limits beyond which deviations from the collapsed curves could be discerned.

In Fig. 10 we show the results of the scaling procedure for $(Fe_{0.68}Mn_{0.32})_{75}P_{16}B_6Al_3$ in the higher temperature regime. The collapse of the isotherms onto two branches $m_\pm^*$ exhibits the critical behavior described by Eq. (9) with a transition temperature $T_c=100(\pm 2)$ K and critical exponents $\beta=0.4(\pm 0.04)$ and $\delta=5(\pm 0.4)$. The demagnetization factor affects the quality of the collapsing for external fields below 100 G and these fields are not shown in Fig. 10. To compare this scaling result with the more conventional Arrott plot technique we show in Fig. 11 a plot of $M^{1/\beta}$ vs $(H/M)^{1/\gamma}$ for various isotherms above and below T_c, using $\beta=0.4$ and $\gamma=\beta(\delta-1)=1.6$. As expected, the isotherms are described by parallel straight lines and the transition temperature is clearly close to 100 K. Magnetization

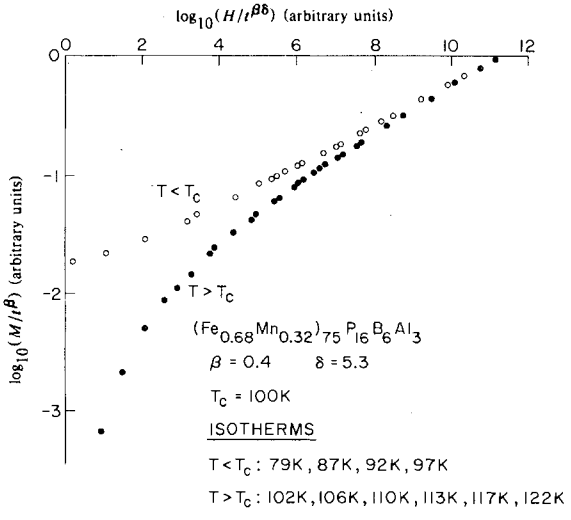

FIG. 10. Scaled magnetic data for the PF transition in $(Fe_{0.68}Mn_{0.32})_{75}P_6B_6Al_3$.

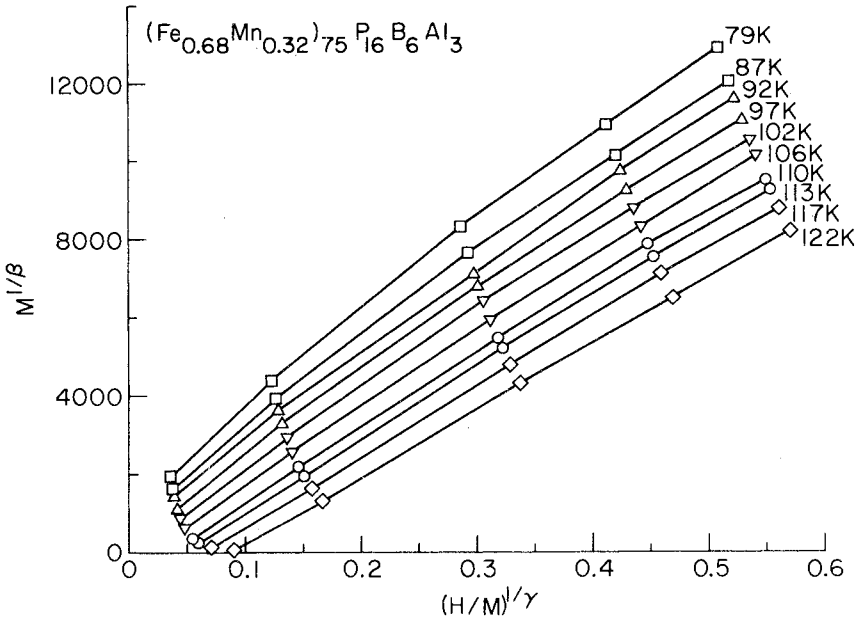

FIG. 11. Arrott plot for isotherms near T_c in $(Fe_{0.68}Mn_{0.32})_{75}P_{16}B_6Al_3$.

results for fields smaller than 100 G are not shown in Fig. 11.

As a second example of the scaling procedure, we show in Fig. 12 the scaling results for $(Fe_{0.20}Ni_{0.80})_{75}P_{16}B_6Al_3$. The same procedure was applied to all FM transitions shown in the phase diagram of Fig. 3. In Table II we summarize the scaling results for all the FM transitions under study. From this table it is clear that for the present amorphous alloys $\beta \simeq 0.4$ and $\delta \simeq 5$. However, it is important to note interesting changes in critical behavior along the PF line as the MCP is approached. We find a scaling behavior similar to Eqs. (8) and (9) but with a single branch and $\delta \simeq 2.2$. For more details see Ref. 22.

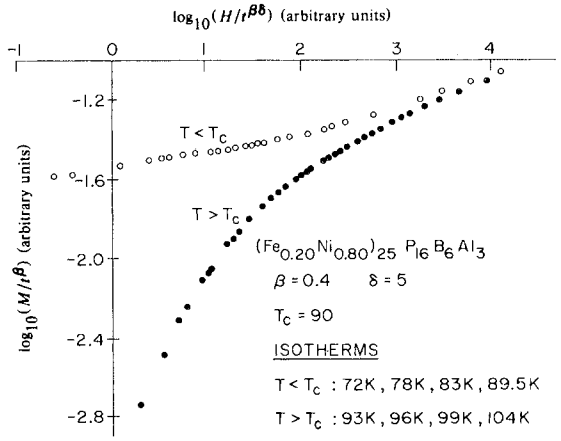

FIG. 12. Scaled magnetic data for the PF transition in $(Fe_{0.20}Ni_{0.80})_{75}P_{16}B_6Al_3$.

VI. FERROMAGNETIC–SPIN-GLASS LINE

In Sec. IV we described experimental results which suggest a transition from a ferromagnetic phase to spin-glass behavior. These include: (i) a drop in the ac susceptibility from its saturated ferromagnetic value at T_d, (ii) a decrease of the low-field dc magnetization at low temperatures, (iii) changes in coercive fields, and (iv) the onset of time-dependent effects. Although these phenomena are indicative of a FM-SG transition, they do not establish the presence of a critical line separating these phases. In this section we demonstrate the existence of such a line and study its critical behavior, using the same scaling procedure described in the previous section. Since the SG phase has $m = 0$, to approach the FM phase from lower temperatures is completely analogous to approaching it from the paramagnetic phase; it is only necessary to reverse the sense of temperature. Equations (8) and (9) still hold, but with t now defined as $\tilde{t} = 1 - T/T_{FG}$ and with new exponents $\tilde{\beta}$ and $\tilde{\delta}$.

In Fig. 13 we show results of this scaling procedure for $(Fe_{0.68}Mn_{0.32})_{75}P_{16}B_6Al_3$. The collapse of the isotherms onto two branches $m_{\pm}$ exemplifies critical behavior in accordance with Eqs. (9) with a transition temperature $T_{FG} = 38(\pm 1)$ K and critical exponents $\tilde{\beta} = 0.4(\pm 0.03)$ and $\tilde{\delta} = 4.5(\pm 0.3)$. As a second example we show in Fig. 14 the scaling results for $(Fe_{0.20}Ni_{0.80})_{75}P_{16}B_6Al_3$ alloy. In this case we find $T_{FG} = 21(\pm 2)$ K, $\tilde{\beta} = 0.5(\pm 0.04)$, and $\tilde{\delta} = 3(\pm 0.3)$. In comparing Figs. 10 and 12 with Figs. 13 and 14 the reader should keep in mind that the temperature

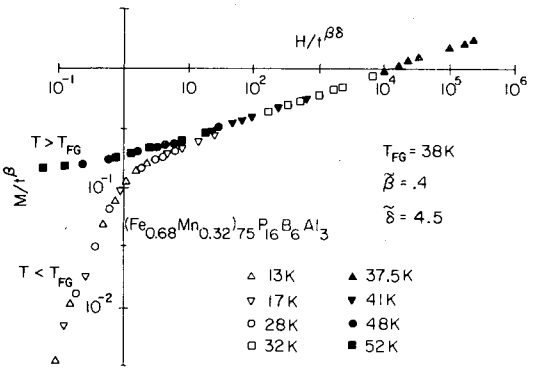

FIG. 13. Scaled magnetic data for the FG transition in $(Fe_{0.68}Mn_{0.32})_{75}P_{16}B_6Al_3$.

axis is reversed. In Figs. 10 and 12 the upper branch describes isotherms *below* T_c while in Figs. 13 and 14 it describes isotherms *above* T_{FG}. (The isotherms in both cases are in the FM regime.) Here, as along the PF line, the values and error bars represent the range of acceptable collapsing of all the data. We must point out that the situation is not so clear along the FG line, since we have no *a priori* reason to believe that scaling should hold.

As in the FM case, the demagnetization factor affects the quality of the collapsing for external fields below 100 G. This limits the use of the scaling demonstration of the FM-SG transitions. As described in Sec. IV, the maximum in the magnetization of the FM alloys decreases to temperatures below our range of measurement in relatively low fields for alloys with smaller values of x. For these alloys it is very difficult to locate the transition and to explore the critical behavior. In Table II we summarize the results of the scaling analysis for alloys on the FG line.

As a concluding remark to this section we note that the drop in the ac susceptibility occurs at temperature $T_d > T_{FG}$.[13] This is illustrated by the dotted line in the phase diagram of Fig. 15 which describes the loci of T_d's for Fe-Mn alloys. The difference between T_{FG} and T_d is a result of the opening of hystersis loops[7] which affects the ac signal amplitude, as will be discussed in Sec. VIII.

VII. SPIN-GLASS LINE AND MULTICRITICAL POINT

The single most characteristic feature of the spin-glass transition is the appearance of a cusp in the low-field susceptibility χ. In the present systems, this low-field cusp must evolve into an infinite peak as the ferromagnetic phase is approached, since the ferromagnetic phase is bounded by lines along which χ diverges. In this section we discuss this change in the susceptibility maxima as the composition approaches the ferromagnetic range.

In Fig. 16, we plot the ac-susceptibility peaks for the Fe-Mn system from Ref. 6. In our earlier analysis, the position of the ferromagnet–spin-glass line was not known, and this led to an only approximately correct analysis of the behavior of the spin-glass transition. Our present understanding of the phase diagram of the Fe-Mn system requires a reanalysis of the susceptibility data, making use of the proper position of the MCP and of the FG line. The analysis follows the lines used previously, but with the scaling axes redefined (Fig. 15) to correspond to the complete phase diagram. The axis $g=0$ is chosen to pass through the MCP and be tangent to the FG line. Thus, an approach to the MCP along $g=0$ will not enter either the ferromagnetic or spin-glass phases, and would give true multicritical behavior. A second axis $\mu=0$ is tangent to the PF line at the MCP. The multicritical point is taken to

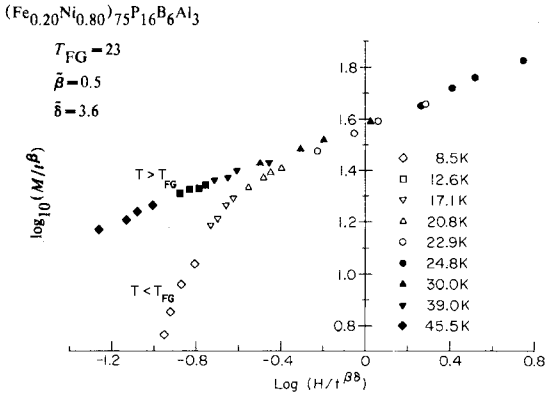

FIG. 14. Scaled magnetic data for the FG transition in $(Fe_{0.20}Ni_{0.80})_{75}P_{16}B_6Al_3$.

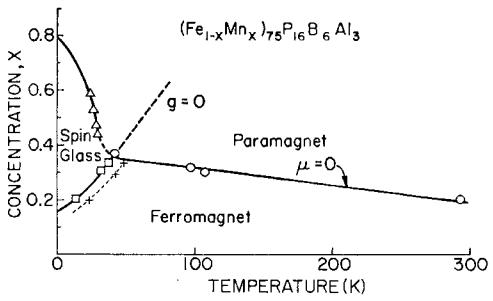

FIG. 15. Phase diagram for $(Fe_{1-x}Mn_x)_{75}P_{16}B_6Al_3$ with definition of g and μ fields used for scaling the susceptibility data. The dotted line describes the loci of T_d in ac susceptibility measurements.

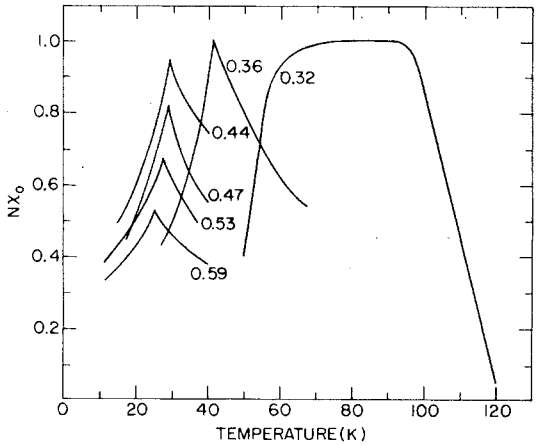

FIG. 16. Low field ac susceptibility for $(Fe_{1-x}Mn_x)_{75}P_{16}B_6Al_3$.

be a $x_{MCP}=0.36$ and $T_{MCP}=41$ K; this temperature differs slightly from the dc data due mainly to slight temperature errors in the ac apparatus. With this choice, the scaling axes are defined to be

$$g=(x/x_{MCP}-1)-0.7(T/T_{MCP}-1) \tag{10}$$

and

$$\mu=(T/T_{MCP}-1)+7.5(x/x_{MCP}-1)\ . \tag{11}$$

If, as we assume here, the line of spin-glass transitions is a critical line, it can be expressed in terms of a crossover exponent ϕ as

$$\mu_{PG}=kg_{PG}^{1/\phi}\ , \tag{12}$$

where the subscript refers to the values of the scaling fields along the paramagnetic–spin-glass line. In Fig. 17 we have plotted the positions of the peaks in the ac susceptibility, converted to the (g,μ) coordinate system. Equation (12) is satisfied with $1/\phi=1.35\pm0.1$ and $k\cong1.0$.

Because the PG line acts as a critical line, we may make a scaling hypothesis about the way in which the susceptibility approaches the MCP. We must keep in mind that χ is *not* critical along this line, but has a singularity only at the MCP. Thus, we may write

$$\chi(T,x)=g^{-\gamma_t/\phi}\chi^*(\mu/g^{1/\phi})\ . \tag{13}$$

This hypothesis may be tested by plotting $\chi/g^{-\gamma_t/\phi}$ vs the scaling variable $\mu/g^{1/\phi}$ for a suitably chosen value for the tricritical susceptibility exponent γ_t. Such a plot is shown in Fig. 18 for which $\gamma_t=1.1\pm0.1$. Thus, we have the same value of ϕ as previously, but now obtain a tricritical exponent γ_t much closer to a mean-field-like value. Indeed, examination of Eq. (2) leads to a prediction that $\gamma_t=1$ and $\delta_t=2$, both of which appear to be borne out by our data. The crossover exponent, however, differs from its mean-field value.

There are a number of difficulties in treating ac susceptibility data in this way, the most serious of which is the need to convert measured susceptibility using the demagnetizing factor. We have used the same demagnetizing factor for all samples, but chose it to lead to a divergence at $x=0.36$. This is reasonable since all concentrations lower than $x=0.36$ show characteristically flattened tops of comparable magnitude as shown in Fig. 16. Further tests of scaling along the spin-glass line are clearly needed before this can be definitively classified as a true phase transition.

The interpretation of ac susceptibility data becomes increasingly difficult with larger concentrations and within the ferromagnetic temperature regime. This is because the ac method measures the reversible magnetization, not the susceptibility, of a ferromagnet, and is therefore extremely sensitive to the nature of the hysteresis loop. Sufficiently close to the MCP,

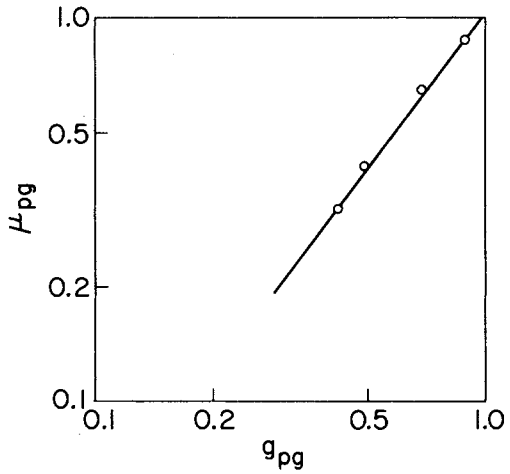

FIG. 17. Locus of susceptibility cusps in the g-μ coordinate system, cf. Eq. (12).

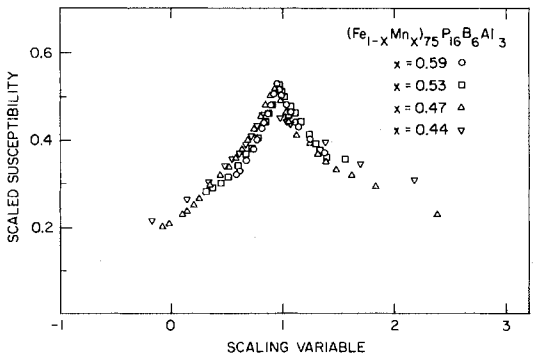

FIG. 18. Susceptibility along the SG line scaled according to Eq. (13). The axes are defined by Eqs. (10) and (11).

the ferromagnetic regime is narrow in temperature, and we may still hope to use ac susceptibility data to locate the phase boundaries

As noted above in regared to Fig. 4, the ac signal for concentrations close to the MCP gives a broadened maximum rather than a sharp peak. The application of a small dc field can split the peak enabling us to resolve two transitions. As we[22] and others[23] have pointed out, the scaling properties of the PF transition cause the maximum in the susceptibility signal to move to higher temperatures in step with the applied field so as to keep the ratio $H/t^{\beta\delta}$ constant. Since we have asserted that scaling holds also at the FG transition, we should expect $H/\tilde{t}^{\tilde{\beta}\tilde{\delta}}$ to remain constant as well which, from the definitions of t and $\tilde{t}$ means that the peaks will separate as H is increased. This effect is illustrated by Fig. 4. The reader must keep in mind that this procedure is valid only so long as the ac modulation exceeds the coercive field. Otherwise, we measure only sequences of minor hysteresis loops which are moved along the magnetization curve of the ferromagnet. This makes the determination of the lower transition by this method risky, at best.

VIII. DISCUSSION

We have reported here the detailed magnetic behavior of a number of amorphous alloys in which the glass-forming components are kept identical. This enables us to study the alloying effects independent of changes induced by the addition of metalloids needed for glass formation. What is more, we can make alloys over ranges of composition not accessible within single, crystalline phases. The major results of this work may be summarized as follows:

(1) All mixed transition-metal alloys studied have a reentrant ferromagnetic regime bounded by a spin-glass-like phase and the paramagnetic phase.

(2) A multicritical point has been located for each alloy system, at the juncture of ferromagnetic, spin-glass, and paramagnetic phases.

(3) Between ferromagnetic and spin-glass phases in each system a line of transitions has been identified along which the magnetization tends to vanish and the susceptibility, to deverge.

(4) Critical exponents along the ferromagnetic line, but not too far from the MCP, have values unlike Heisenberg (or other n-component systems) in 3D.

(5) Critical exponents have been extracted for the FG lines, and for Fe-Mn alloys these are quite simialr to 3D Heisenberg values. Different values are obtained for different systems (Table II) but this seems to be due to a different "distance," $(x_{\mathrm{MCP}}-x)/x_{\mathrm{MCP}}$, from MCP.

(6) The PG line of spin-glass transitions can also be viewed as a critical line insofar as the peaks in the susceptibility tend to grow systematically, and in an appropriate scaling manner as the MCP is approached.

(7) The MCP itself looks surprisingly similar to that predicted by the Sherrington-Kirkpatrick model for spin-glass behavior.

(8) The FG critical line as determined by scaling is consistently at lower temperature than that which would be obtained from ac susceptibility studies. This discrepancy is being studied in greater detail and will be reported elsewhere.

From the point of view of the phase diagram and critical behavior, Fe and Co appear to be interchangeable, although the PG line for the Co-Mn system is anomalous. Ni and Mn, to the contrary, behave very differently. Ni appears to act mainly as a nonmagnetic diluent in these alloys, with the MCP quite close to the percolation limit $x=0.2$ in 3D. The presence of a spin-glass regime extending to significantly lower Fe or Co concentrations would indicate that Ni atoms maintain some magnetic properties. Mn, on the other hand, seems to be almost ideal as an antiferromagnetic addition, with the MCP not far from the $x=0.5$ expected for equal and opposite exchange interactions. The shift in the MCP toward the Fe- or Co-rich end probably is a result of the antiferromagnetic Mn-Mn interaction which also abets spin-glass formation. An interesting exercise would involve the study of a three-δ-function which model with appropriate Fe-Fe (Co-Co), Mn-Mn, and Mn-Fe (Co) exchange constants. Such a approach was introduced in Ref. 24 to account for the different slopes of the PG lines.

One of the most intriguing aspects of the present work is the nature of the low-temperature phase of those ferromagnets which are reentrant. From our scaling analysis, we have located the transition temperatures while avoiding the complications of an open hysteresis loop. The difference between this low-temperature phase and a ferromagnet is a subtle one. It involves the onset of a decaying remanence and a magnetization which grows more slowly with increasing field at low temperature than it would for a ferromagnet. All, or at least most, of the phenomena can be found in the technical magnetic properties of many alloys. Great care must be taken, for example, not to mistake a slowly rising virgin magnetization curve for nonferromagnetic behavior. The pitfalls of using changes in ac induction experiments to signal the lower phase transition have already been amply debated in the literature. It is our view that the combination of these various effects, coupled with the strong evidence for scaling behavior, points to a phase transition from ferromagnetic behavior to a spin-glass-like phase. Further work is necessary to determine that this low-temperature phase is continuous with the spin-glass region reached by crossing the PG line.

Having established the presence of a MCP and reentrant ferromagnetic regime, we still must face the issue of the spin-glass phase itself. Is the PG line really a line of phase transitions? We have demonstrated that the susceptibility cusps satisfy a scaling law along this curve, but that could simply imply that the PG line is a natural scaling direction for the MCP, rather than a distinct critical line. Indeed, this interpretation has been recently offered by Morgenstern and Binder,[25] who have found that the PG line, in Monte Carlo simulations, does not act as a critical line should. He suggests that the MCP is a special point at which $dT_c(x)/dx$ vanishes, and the FG line is governed by a percolation MCP at zero temperature. In this picture, the spin-glass phase is continuous with the paramagnetic regime. We cannot, from our present results, distinguish this picture from the Sherrington-Kirkpatrick phase diagram. It is both an intriguing path out of difficulties associated with the spin-glass model, and a disappointment if the spin-glass turns out to be only a syrupy paramagnet.

ACKNOWLEDGMENTS

It is a pleasure to thank Barnett Kramer for continuous assistance with the ac susceptibility apparatus and John Woodhouse for his electron microprobe measurements. We wish to thank E. Figueroa, K. Gramm, and Professor Beckman, University of Uppsala, Sweden, for making available to us some of their unpublished data. This research was supported in part by the National Science Foundation under MRL Grant No. DMR-77-23999.

*Present address: Central Research Laboratory, 3M Center, St. Paul, Minn. 33221.

[1]S. Kirkpatrick and D. Sherrington, Phys. Rev. B 17, 4384 (1978); M. W. Klein, L. J. Schowalter, and P. Shukla, Phys. Rev. B 19, 1492 (1979); S. Fishman and A. Aharony, *ibid.* 21, 280 (1980).

[2]A. J. Bray and M. A. Moore, J. Phys. C 13, 419 (1980), and references therein.

[3]R. D. Shull, H. Okamoto, and P. A. Beck, Solid State Commun. 20, 863 (1976).

[4]B. H. Verbeek, G. J. Nieuwenhuys, H. Stocker, and J. A. Mydosh, Phys. Rev. Lett. 40, 586 (1978).

[5]K. V. Rao, R. Malmhäll, S. M. Bhagat, G. Bäckström, and H. S. Chen, Proc. IEEE Trans. Magn. MAG 16, 896 (1980); S. M. Bhagat, J. A. Goehegan and H. S. Chen, Solid State Commun. 36, 1 (1980).

[6]M. B. Salamon, K. V. Rao, and H. S. Chen, Phys. Rev. Lett. 44, 596 (1980).

[7]D. W. Carnegie and H. Claus, Phys. Rev. B 20, 1280 (1979); J. A. Mydosh, G. J. Nieuwenhuys, and B. H. Verbeek, Phys. Rev. B 20, 1282 (1979).

[8]H. Maletta and Y. Convert, Phys. Rev. Lett. 42, 108 (1979).

[9]D. Hüser, G. Daub, M. Gronau, S. Methfessel, and D. Wagner, J. Magn. Magn. Mater. 15–18, 207 (1980).

[10]C. R. Fincher, S. M. Shapiro, A. H. Palumbo, and R. D. Parks, Phys. Rev. Lett. 45, 474 (1980).

[11]J. W. Lynn, R. W. Erwin, J. J. Rhyne, and H. S. Chen, J. Appl. Phys. 52, 1738 (1981).

[12]S. M. Bhagat, M. L. Spano, and K. V. Rao, J. Appl. Phys. 50, 1580 (1979).

[13]Y. Yeshurun, M. B. Salamon, K. V. Rao, and H. S. Chen, Phys. Rev. Lett. 45, 1366 (1980).

[14]S. F. Edwards and P. W. Anderson, J. Phys. F 5, 965 (1976).

[15]M. Wortis, C. Jayaprakash, and E. K. Riedel, J. Appl. Phys. 49, 1335 (1978).

[16]J. H. Chen and T. C. Lubensky, Phys. Rev. B 16, 2106 (1977).

[17]See, for example, H. G. Stanley, *Introduction to Phase Transition Critical Phenomena* (Oxford Univ. Press, New York, 1971).

[18]H. S. Chen and C. E. Miller, Mater. Res. Bull. 11, 49 (1976).

[19]R. C. Sherwood, E. M. Gyorgy, H. S. Chen, S. D. Ferris, G. Norman, and H. J. Leamy, in *Magnetism and Magnetic Materials—1974 (San Francisco),* edited by C. D. Graham, G. H. Lander, and J. J. Rhyne, AIP Conf. Proc. No. 24 (AIP, New York, 1974) p. 745.

[20]D. R. Rhiger, D. Müller, and P. B. Beck, J. Magn. Magn. Mater. 15, 165 (1980).

[21]Y. Yeshurun, K. V. Rao, M. B. Salamon, and H. S. Chen, J. Appl. Phys. 52, 1747 (1981).

[22]M. B. Salamon, K. V. Rao, and Y. Yeshurun, J. Appl. Phys. 52, 1687 (1981).

[23]P. Gaunt, S. C. Ho, G. Williams, and R. W. Cochrane, Phys. Rev. B 23, 251 (1981).

[24]K. Moorjani, S. K. Ghatak, K. V. Rao, and B. Kramer, J. Phys. (Paris) 41, C8-718 (1980).

[25]I. Morgenstern and K. Binder, J. Appl. Phys. 52, 1692 (1981).